

A Mutant Mouse with Severe Anemia and Skin Abnormalities Controlled by a New Allele of the Flaky Skin (*fsn*) Locus

Shuji TAKABAYASHI¹⁾ and Hideki KATOH^{1, 2)}

¹⁾Institute for Experimental Animals, Hamamatsu University School of Medicine, 1–20–1 Handayama, Hamamatsu, Shizuoka, 431-3192, and ²⁾Central Institute for Experimental Animals 1430 Nogawa, Miyamae-ku, Kawasaki, Kanagawa, 216-0001, Japan

Abstract: We found a novel recessive mutation in an inbred strain, INT, that was derived from an ICR closed colony. Mice homozygous for this mutation are identified by severe anemia, dysgenesis and neonatal death. This mutation was tentatively named *int*. Intercrosses of *int* heterozygotes (+/*int*) and the flaky skin heterozygotes (+/*fsn*) resulted in abnormal mice (*int/fsn* heterozygotes) showing anemia and flaky skin with the expected frequency for autosomal recessive mutation. The *int* gene was therefore named *fsn*^{Jic} as an allele of the *fsn* locus on chromosome 17. We carried out phenotype analyses using B6.INT- *fsn*^{Jic} mice to observe phenotypes of blood and skin in the embryonic and neonatal stages. Discrimination of *fsn*^{Jic} embryos from normal embryos was performed by an indirect diagnosis of the *fsn*^{Jic} gene using the D17Mit130 microsatellite marker tightly linked to the *fsn* locus. The number of fetal nucleated RBC of normal embryos decreased gradually to 17.5 dpc, but that of the abnormal embryos decreased to 14.5 dpc followed by a gradual increase to 17.5 dpc. Skin of *fsn*^{Jic} embryos did not show any abnormalities and expressed cytokeratins normally as skin epithelial cell markers at each embryonic stage (15.5 dpc to 18.5 dpc). Time differences in the appearance of the different phenotypes observed in various tissue and organs of *fsn* homozygotes suggest they are caused by expression of the *fsn* gene at different developmental stages.

Key words: anemia, dysgenesis, flaky skin, *fsn* gene, ICR

Introduction

It is known that many spontaneous mutations have been found in inbred strains derived from closed colonies of mice, e.g. NOD/Shi [9] and III/Jic [3, 4, 6]. In 1986, we found a novel recessive mutation identified

by severe anemia and early death within 10 days of birth in the INT strain derived from a Jcl:ICR closed colony [5]. We tentatively named this mutation *int*, the same name as the strain. Genetic studies performed so far have revealed that this is an autosomal recessive mutation and that it is mapped to the distal region of

(Received 3 September 2004 / Accepted 25 May 2005)

Address corresponding: H. Katoh, Institute for Experimental Animals, Hamamatsu University School of Medicine, 1–20–1 Handayama, Hamamatsu, Shizuoka 431-3192, Japan

chromosome 17.

An autosomal recessive mutation designated flaky skin (*fsn*) was found at the Jackson Laboratory (ME, USA). The *fsn* homozygous neonates show anemia and adult *fsn* homozygotes show a patchy, thick and white scale skin at about 4 weeks of age. Phenotypes of *fsn* homozygotes are associated with abnormalities of stratified squamous epithelia and the hematopoietic system. The *fsn* mutation was mapped to the distal region of chromosome 17 [1, 11, 15].

We noted similarities of the phenotypes in both *int* and *fsn* homozygotes described above. So far, we have attempted to demonstrate that these mutations are alleles of the *fsn* locus. In this paper, we describe the genetic relation between *int* and *fsn* genes demonstrated by linkage analyses and allelism tests. We also report the histological and hematological phenotypes of the affected mice homozygous for the *int* gene at the embryonic stages.

Materials and Methods

Animals and genetic crosses

A novel recessive mutation (tentatively named *int*) that occurred spontaneously was found in an inbred strain, INT, established from a Jcl:ICR closed colony at the Central Institute for Experimental Animals (Kawasaki, Japan). Mice homozygous for the *int* mutation were identified by pallor due to severe anemia at birth and skin abnormalities at about 10 days after birth.

Three *int* congenic strains, B6.INT-*int* (N8 in 2004), CBy.INT-*int* (N5 in 2004) and C3.INT-*int* (N5 in 2004), were bred using C57BL/6Jcl (B6), BALB/cByJcl (CBy) and C3H/HeNJcl (C3) mice purchased from CLEA Japan (Tokyo, Japan). An intercross-backcross system was adapted to establish these congenic strains.

Hematological and histological studies were performed to describe the phenotypes of *int* homozygotes in the embryonic and neonatal stages. Intercrosses of B6.INT-*int* heterozygotes (+/*int*) were carried out to obtain the *int* homozygotes at 12.5, 13.5, 14.5, 15.5, 16.5, 17.5 and 18.5 dpc (days post-coitus). Observation of a vaginal plug on the morning after pairing determined the embryonic stage as 0.5 dpc. Genotypes of the *int* gene in embryos were determined using the *D17Mit130* microsatellite marker as described below.

To demonstrate allelism of *int* and *fsn* genes, crosses

of B6.INT-*int* (+/*int*) and CBy.A-*fsn* (+/*fsn*) purchased from the Jackson Laboratory (ME, USA) were performed. A fine map of chromosome 17 was drawn based on the results of linkage analyses using F₂ progeny obtained by intercrosses of (B6.INT-+/*int* and C3H/HeNJcl-+/+)F₁-+/*int* mice.

Microsatellite markers for fine mapping

For fine mapping and indirect diagnosis of the *int* gene, we developed four Ham (Laboratory code for Hamamatsu University School of Medicine) microsatellite markers detected as SSLPs (simple sequence length polymorphisms) on chromosome 17 as follows: *D17Ham2* (forward: tggcccagcaagtaatgacaac, reverse: tgggctggtaaatggaccttc), *D17Ham9* (forward: actggacttcaccaacag, reverse: gctcaaacgcttttcgac) and *D17Ham34* (forward: ttgtactggtgatgctcct, reverse: ctggagagacaactcatcca). These primers were designed using DNA sequences obtained from the NCBI database. Other primers for microsatellite markers used in this study were purchased from Invitrogen (CA, USA).

Genomic PCR and RT-PCR

Using a standard phenol-chloroform method, genomic DNA was prepared from various tissues, depending on the experiments, and used as template DNA for PCR. Amplification of microsatellite markers by PCR was performed under the following conditions: 30 cycles of DNA degeneration for 20 s at 94°C, annealing for 30 s at 57°C and extension for 40 s at 72°C. PCR products were electrophoresed on 3% agarose gel followed by staining with ethidium bromide and the results were photographed.

RT-PCR was performed in order to observe expressions of *Hbb-bhl* (hemoglobin Z, beta-like embryonic chain) and *Hbb-bl* (hemoglobin, beta adult major chain) genes as the markers of erythrocyte maturity [8]. Total RNA was extracted from livers of 14.5 dpc embryos using RNeasy (Qiagen, MD, USA) according to the manufacturer's instructions. One microgram of total RNA was reverse-transcribed using oligo-dT primer and superscript II RT (Gibco BRL, MD, USA). cDNA was amplified under the following conditions: 30 cycles of DNA degeneration for 1 min at 94°C, annealing for 1 min at 60°C, and extension for 1 min at 72°C. Primer sequences used in this study were as follows: *Hbb-bhl* (forward: ctcaaggagacctttgctca, reverse:

agtccccatggagtcaaaga) and *Hbb-b1* (forward: cacaaccccagaacagaca, reverse: ctgacagatgctctcttggg).

Histology and Hematology

Blood was collected in heparinized microhematocrit tubes (Drummond, PA, USA) for hematological studies. Red blood cells (RBC), white blood cells (WBC) and platelets (PLT) were counted with an automated hematology analyzer, SF-3000 (Sysmex, Hyogo, Japan). In order to observe various blood cells, blood smears were prepared and stained with Wright-Giemsa solution. The number of FNRBC (fetal nucleated red blood cells) per square millimeter was counted using NIH Image software (version 1.62 available at <http://rsb.info.nih.gov/nih-image/download.html>).

Tissue samples were collected and fixed in Bouin's solution overnight followed by embedding in paraffin and sectioning at 5 μ m. Sections were stained with hematoxylin and eosin (HE) and observed under a light microscope (Olympus, Tokyo, Japan). Staining procedures for immunohistochemical studies were as previously described [15, 16]. Briefly, sections prepared from embryos were stained using a panel of polyclonal rabbit antibodies specific for mouse keratinocyte markers (K1, K6 and K14) [9, 10] with the ABC kit (Vector, CA, USA) according to the manufacturer's instructions. They were counterstained with hematoxylin.

Microbiological monitoring and approval of animal experimentation

Microbiological monitoring was performed by our in-house monitoring system every three months to determine microbiological conditions in the animal rooms. Samples collected from mice used in this study were sent to the ICLAS Monitoring Center (Kawasaki, Japan) to check for as many microorganisms as possible. No infection was detected in any animal room in which the mice used in this study were maintained.

The experimental protocol and design were approved by the Animal Experimentation Committee and performed according to the Guidelines for Animal Experimentation of Hamamatsu University School of Medicine.

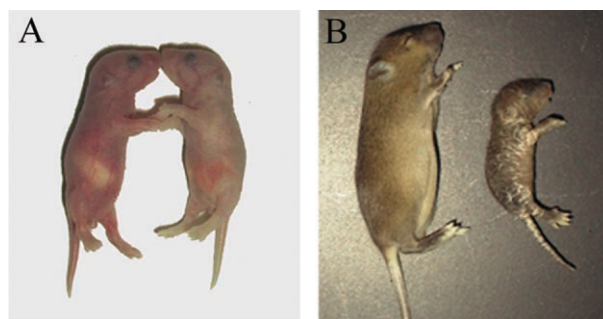


Fig. 1. Mice of congenic strains with a novel mutation showing severe anemia and skin abnormalities. (A) B6.INT-*int* (=f5n^{Jic}) mice at one day after birth (Right: affected mouse, Left: normal mouse). (B) C3.INT-*int* (=f5n^{Jic}) mice at 10 days after birth (Right: affected mouse, Left: normal mouse).

Results

Establishment of three *int* congenic strains

We bred three congenic strains of *int* gene to study phenotypes of the *int* gene on genetic backgrounds of C57BL/6JJcl, BALB/cByJJcl and C3H/HeNJcl mice.

The first congenic strain was B6.INT-*int*. The mean life span of affected mice (B6.INT-*int/int*) was 3.5 \pm 0.6 days (N=15). An affected mouse one day after birth is shown in Fig. 1A (right) and a normal littermate (B6.INT-+/? : B6.INT-+/*int* or +/+) in Fig. 1A (left). Affected mice were distinguished from normal mice by abnormal phenotypes of pale skin caused by anemia and lined tails.

The second congenic strain is CBy.INT-*int* (picture not shown). The mean life span of affected mice (CBy.INT-*int/int*) was 7.7 \pm 0.8 days (N=9). Affected mice showed severe anemia and papulosquamous skin lesions.

The third congenic strain is C3.INT-*int*. The mean life span of the affected mice (C3.INT-*int/int*) was 11.6 \pm 0.5 days (N=7). An affected mouse at 10 days after birth is shown in Fig. 1B (right) and a normal littermate (C3.INT-+/? : +/*int* or +/+) in Fig. 1B (left). Affected mice showed severe anemia and papulosquamous skin lesions, the same as observed in the CBy.INT-*int* congenic strain.

The mean life span of the B6.INT-*int/int* mice was shorter than those of the other *int* congenic strains. A marked effect of genetic backgrounds on phenotypes of the *int* mutation was observed with the mean life span.

Inheritance of the *int* gene and allelism tests

During breeding of the three *int* congenic strains, intercrosses of *int* heterozygotes were performed to confirm inheritance of the *int* mutation. With the B6.INT-*int* congenic strain, 65 mice were obtained from seven litters. Fifteen (23.1%) mice were *int* homozygotes (9 females and 6 males). With the CBy.INT-*int* congenic strain, 25 mice were obtained from four litters, and 6 (24.0%) were *int* homozygotes (4 females and 2 males). With the C3.INT-*int* congenic strain, 123 mice were obtained from 20 litters, and 33 (26.8%) were *int* homozygotes (17 females and 16 males). Since these incidences of *int* homozygotes were identical to the incidences expected in a recessive mutation, we consider that the *int* gene reported in this paper is an autosomal recessive mutation.

To study allelism of the *int* and *fsn* genes, 37 F₁ mice were obtained by mating B6.INT-+/+*int* and CBy.A-+/+*fsn*. Nine (24.3%) of them showed abnormal phenotypes and 28 normal phenotypes. This incidence was identical to that (25%) expected in a recessive mutation. Therefore, it was concluded that the *int* gene is an allele of the *fsn* gene and it was tentatively named *fsn^{Jic}* according to the gene nomenclature guideline (<http://www.informatics.jax.org/mgihome//nomen/gene.shtml>). The mean life span of *fsn/int* (*fsn^{Jic}*) mice was 67.2 ± 3.6 days (N=9). In contrast, the mean life span of *fsn* homozygous mice (CBy.A-*fsn/fsn*) was 97.8 ± 44.8 days (N=11).

Fine map around the *fsn^{Jic}* gene on chromosome 17

Figure 2 shows the fine map around the *fsn^{Jic}* (*int*) gene on chromosome 17 drawn from the results obtained in this study. Among the Ham (Hamamatsu University School of Medicine) microsatellite markers, *D17Ham9* was mapped between *D17Mit190* and *D17Mit129*, and both *D17Ham34* and *D17Ham2* were mapped between *D17Mit130* and *D17Mit221*.

The *fsn^{Jic}* gene was precisely assigned to the distal region of chromosome 17 using 211 *fsn^{Jic}* F₂ mice obtained by intercrosses of (C3H/HeJ-+/+ × B6.INT-+/+*fsn^{Jic}*)F₁-+/+*fsn^{Jic}*. No recombinants (0/422 chromosomes) between *fsn^{Jic}* and *D17Mit130* genes were observed. Recombination frequencies between *fsn^{Jic}* and *D17Mit129* genes and between *fsn^{Jic}* and *D17Ham34* genes were 0.2% (1/422) and 1.9% (8/422), respectively. These results suggest that the *fsn^{Jic}* gene is

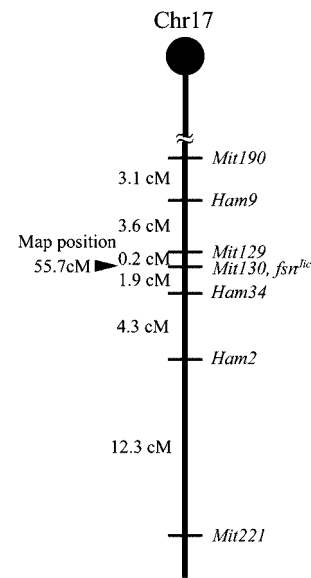


Fig. 2. Fine map of chromosome 17 drawn from the results obtained in this study. No recombinant (0/422 chromosomes) between *fsn^{Jic}* and *D17Mit130* genes was observed. Recombination frequencies between *fsn^{Jic}* and *D17Mit129* genes and between *fsn^{Jic}* and *D17Ham34* genes were 0.2% (1/422) and 1.9% (8/422), respectively. These results suggested that the *fsn^{Jic}* gene is located between *D17Mit129* and *D17Ham34*.

located between *D17Mit129* and *D17Ham34*.

Characterization of the *fsn^{Jic}* neonate

Table 1 shows body weights of normal mice (+/+ or +/*fsn^{Jic}*) and *fsn^{Jic}* homozygotes (*fsn^{Jic}/fsn^{Jic}*) at 10 days of age and ratios of organ weights (mg) to body weights (g) in the C3.INT-*fsn^{Jic}* congenic strain. The average body weight of *fsn^{Jic}* homozygotes was lower than that of normal mice. Compared with ratios of organ weight (mg) to body weight (g) of normal mice, those of *fsn^{Jic}* homozygotes were significantly higher for the heart and spleen, but significantly lower for the thymus. Although data are not shown, we observed markedly reduced white pulp and increased red pulp in spleens of *fsn^{Jic}* homozygotes. We also observed remarkably reduced cortex cellularity in livers of *fsn^{Jic}* homozygotes. Livers and kidneys of *fsn^{Jic}* homozygotes were paler than those of normal mice. Livers of *fsn^{Jic}* homozygotes showed hepatitis with an inflammatory cell infiltrate and marked extramedullary hematopoiesis was observed

Table 1. Body and organ weights of the normal (+/+ or *fsn^{Jic}*) and affected (*fsn^{Jic}/fsn^{Jic}*) neonatal mice (10 days old) of the C3.INT-*fsn^{Jic}* congenic strain

Genotype	No. tested	Body weights (g)	Ratio of organ weight (mg) to body weight (g) (Organ weights (mg) in parenthesis)				
			Heart	Spleen	Thymus	Liver	Kidney
<i>fsn^{Jic}/fsn^{Jic}</i>	7	3.6 ± 0.3	10.1 ± 0.6* (38.9 ± 4.3)	8.8 ± 1.1* (32.8 ± 6.0)	1.6 ± 0.3* (5.6 ± 0.1)	48.9 ± 4.30 (177.1 ± 22)	14.6 ± 0.8 (52.2 ± 4.5)
+/?	8	7.9 ± 0.5	5.9 ± 0.8 (49.9 ± 5.4)	5.7 ± 0.6 (46.9 ± 7.2)	5.2 ± 0.3 (41.1 ± 3.5)	40.0 ± 1.17 (317.7 ± 23)	13.5 ± 1.0 (109.7 ± 8.2)

*Mean value for *fsn^{Jic}/fsn^{Jic}* is significantly different from +/? littermates by t-test at *P*<0.05.

Table 2. Hematologic values of the normal (+/?) and affected (*fsn^{Jic}/fsn^{Jic}*) neonatal mice (10 days old) of the C3.INT-*fsn^{Jic}* congenic strain

Genotype	No. tested	Hct (%)	RBC (× 10 ⁶ /μl)	Nucleated cells (× 10 ³ /μl)	MCV (fl)	MCH (pg)	MCHC (g/dl)	PLT (× 10 ⁴ /μl)
<i>fsn^{Jic}/fsn^{Jic}</i>	5	11.3 ± 2.5**	14.7 ± 3.0**	104.0 ± 11.7**	75.3 ± 2.3	20.5 ± 1.0	27.8 ± 1.9	77.5 ± 8.3*
+/?	10	30.3 ± 0.9	42.7 ± 1.3	3.1 ± 0.3	71.0 ± 0.4	22.2 ± 0.2	31.2 ± 0.2	47.3 ± 5.4

Data are mean ± standard error of the mean. *Mean value for *fsn^{Jic}/fsn^{Jic}* is significantly different from +/? littermates by t-test at *P*<0.01.

**Mean value for *fsn^{Jic}/fsn^{Jic}* is significantly different from +/? littermates by t-test at *P*<0.0001.

in livers and spleens of *fsn^{Jic}* homozygotes (data not shown).

Table 2 shows hematological data of neonates (10 days after birth) of normal and affected mice in the C3H.INT-*fsn^{Jic}* congenic strain. Hct values of *fsn^{Jic}* homozygotes were much lower than average values of normal mice, but the collected blood samples of *fsn^{Jic}* clotted normally at room temperature. The number of RBCs was significantly decreased in *fsn^{Jic}* homozygotes, but the number of nucleated cells was 35 times higher than that of normal mice. The number of platelets (PLTs) was significantly increased in *fsn^{Jic}* homozygotes. The mean corpuscular volume (MCV), mean corpuscular hemoglobin (MCH) and mean corpuscular hemoglobin concentration (MCHC) were almost the same in normal and affected mice.

Figures 3A and 3B show peripheral blood of a normal 10-day-old neonate and an affected 10-day-old neonate, respectively. A considerable number of the RBCs of affected neonates showed abnormalities such as dacryocytes (teardrops) and acanthocytes. Most nucleated cells observed in blood of *fsn^{Jic}* homozygous neonates were erythroblasts. It was difficult to identify types of WBC observed in blood of *fsn^{Jic}* homozygous neonates because broken (smudge) cells [2] were ob-

served. Figures 3C and 3D show skin of a normal neonate and an *fsn^{Jic}* homozygous neonate. As shown in Fig. 3D skin disorders and sparse pelage were observed in *fsn^{Jic}* homozygous neonates with anemia. Skin of 10-day-old *fsn^{Jic}* homozygous neonates showed marked acanthosis and hyperkeratosis with focal parakeratosis and neutrophilic infiltration in epidermis associated with prominent dermal inflammatory infiltrate as shown in Figs. 3D and 3E.

Characterization of *fsn^{Jic}* embryo

In this experiment, the B6.INT-+/+*fsn^{Jic}* congenic strain was used. Genotypes (+/+, +/*fsn^{Jic}* and *fsn^{Jic}/fsn^{Jic}*) of embryos used were indirectly determined using microsatellite markers (*D17Mit190*, *D17Mit129* and *D17Mit130*) closely linked to the *fsn^{Jic}* gene on chromosome 17.

Figure 4A shows the number of fetal nucleated red blood cells (FNRBC) in the peripheral blood of *fsn^{Jic}* homozygous embryos and normal embryos (+/+ or +/*fsn^{Jic}*) at 12.5, 13.5, 14.5, 15.5, 16.5 and 17.5 dpc. The number of FNRBC in normal embryos decreased gradually to 17.5 dpc, but that in *fsn^{Jic}* homozygous embryos decreased to 14.5 dpc followed by a gradual increase to 17.5 dpc. At 17.5 dpc, the number of FNRBC in *fsn^{Jic}*

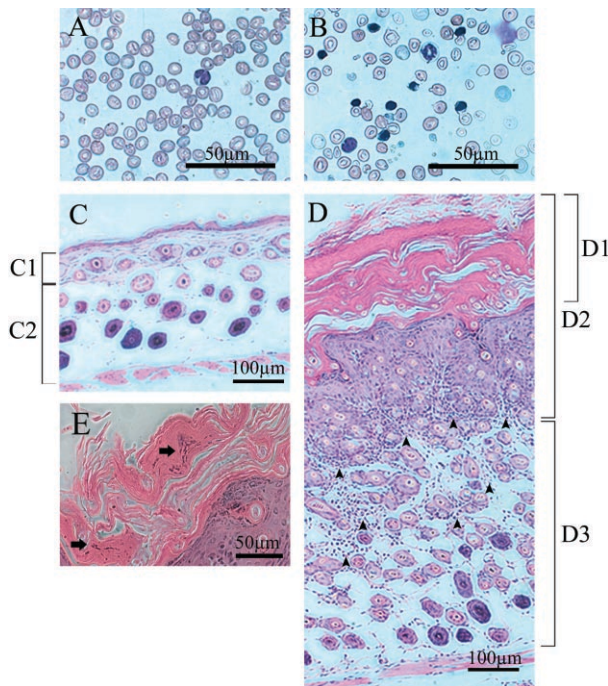


Fig. 3. Blood smears (A and B) and skins (C, D and E) of the normal (C3.INT-+/?: +/+ or +/*fsn^{Jic}*) and affected mice (C3.INT-*fsn^{Jic}/fsn^{Jic}*) at 10 days after birth. (A) Blood smear of the normal mouse (+/?). (B) Blood smear of the affected mouse (*fsn^{Jic}/fsn^{Jic}*). (C) Skin of the normal mouse (+/?); C1: Epidermis, C2: Dermis. (D) Skin of the affected mouse (*fsn^{Jic}/fsn^{Jic}*); D1: Corneal layer of epidermis, D2: Epidermis, D3: Dermis. Neutrophilic infiltration (shown by arrowheads) in the epidermis associated with prominent dermal inflammatory infiltrate was observed. (E) Skin of the affected mouse (*fsn^{Jic}/fsn^{Jic}*). Marked acanthosis and hyperkeratosis with focal parakeratosis was observed as shown by arrows.

embryo was 20 times higher than that of normal embryos. Figure 4B shows blood cells of normal and *fsn^{Jic}* homozygous embryos at 12.5, 13.5, 15.5 and 16.5 dpc. We demonstrated that blood in normal and *fsn^{Jic}* homozygous embryos did not show any histological differences at 12.5 dpc, but the number of FNRBC increased with age (Fig. 4A).

Figure 5 shows dorsal skin sections of normal and *fsn^{Jic}* homozygous embryos at 15.5, 16.5 and 18.5 dpc. Skin of *fsn^{Jic}* homozygous embryos showed no gross histological abnormalities. Figure 6 shows distributions of three keratinocyte markers, K6, K1 and K14, in skin of normal and *fsn^{Jic}* homozygous mice. Periderm was stained with anti-K6 antibody (Figs. 6A and 6B), the upper half of the non-cornified epidermis and

stratum spinosum was stained with anti-K1 (Figs. 6C and 6D) and the lower half of the epidermis and stratum basale was stained with anti-K14 (Figs. 6E and 6F). There was no difference in distribution of the three keratinocyte markers and thickness of the three keratinocyte layers stained between normal and *fsn^{Jic}* homozygous embryos.

Discussion

Mapping data derived in this study show that the *int* (*fsn^{Jic}*) mutation is located between *D17Mit129* and *D17Ham34* and that no recombinant occurred between *fsn^{Jic}* and *D17Mit130*. Therefore, we assumed that the *D17Mit130* marker is useful for indirect diagnosis of genotypes of the *fsn^{Jic}* gene. In this study, we successfully performed various phenotypic analyses using *fsn^{Jic}* homozygous embryos diagnosed for this marker.

Sundberg *et al.* [15] reported that A/J-*fsn* and B6.A-*fsn* exhibit severe phenotypes and die before weaning, while CBy.A-*fsn* mice are mildly anemic at birth and survive until about 3 months of age. In order to obtain *fsn^{Jic}* mice with mild phenotypes and a longer mean life span, we established three congenic strains, B6.INT-*fsn^{Jic}*, CBy.INT-*fsn^{Jic}* and C3.INT-*fsn^{Jic}*. As a result, we observed that phenotypes of B6.INT-*fsn^{Jic}* mice are more severe (mean life span: 3.5 ± 0.6 days) than those of C3.INT-*fsn^{Jic}* mice (mean life span: 11.6 ± 0.5 days). These results reveal that genetic backgrounds have critical effects on phenotypes of the *fsn^{Jic}* gene. The CBy.INT-*fsn^{Jic}* congenic strain with the same genetic background (BALB/cByJ) as the CBy.A-*fsn* congenic strain with a longer mean life span (97.8 ± 44.8 days) showed a short mean life span (7.7 ± 0.8 days). This strongly suggests that the *fsn* and *fsn^{Jic}* genes might have different types of mutations, e.g., insertions or deletions.

Histological studies of *fsn^{Jic}* homozygotes showed severe papulosquamous skin lesions and hematopoietic system disorders as shown in Fig. 1. The *fsn^{Jic}* homozygotes showed enlarged hearts and spleens and reduced weights of thymuses. Beamer *et al.* [2] also observed the same phenotypes in *fsn* homozygotes. The reduced weights in thymuses and the reduced dimensions of the white pulp of spleens in *fsn^{Jic}* homozygotes indicate a decrease in the number of lymphocytes. On the other hand, enlargement of red pulp in spleens of

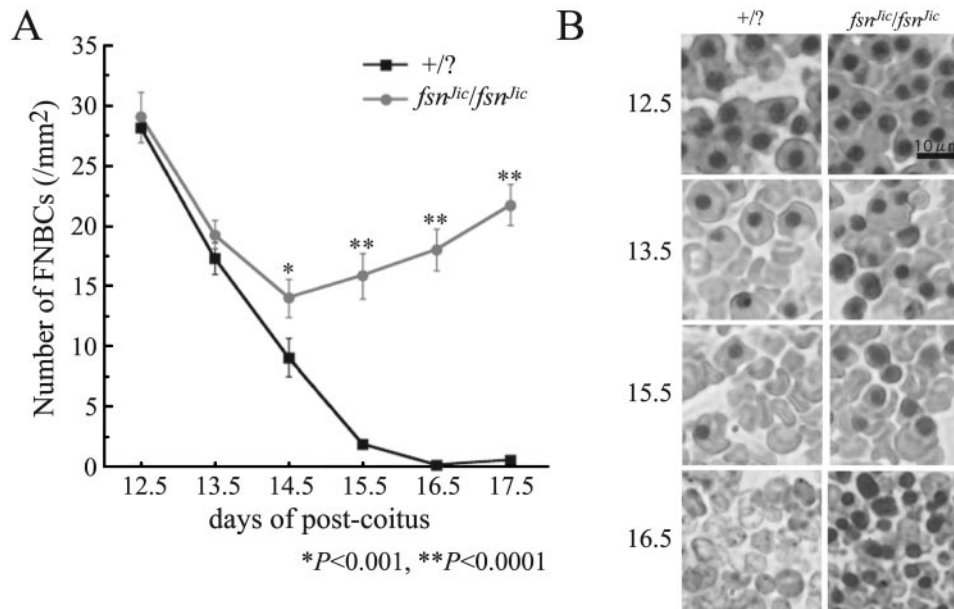


Fig. 4. Phenotypes of fetal nucleated blood cells in the normal and *fsn^{Jic}* homozygous mice at 12.5 dpc to 17.5 dpc. (A) Fetal nucleated red blood cells (FNRC) in the peripheral blood of the normal and affected mouse. The number of FNRC in the affected mice was decreased from 12.5 dpc to 14.5 dpc, but increased gradually to 17.5 dpc. (B) Blood of normal and affected mice. The numbers of nucleated primitive erythrocytes in the peripheral blood of normal and *fsn^{Jic}* homozygous embryos at 12.5 dpc were almost the same.

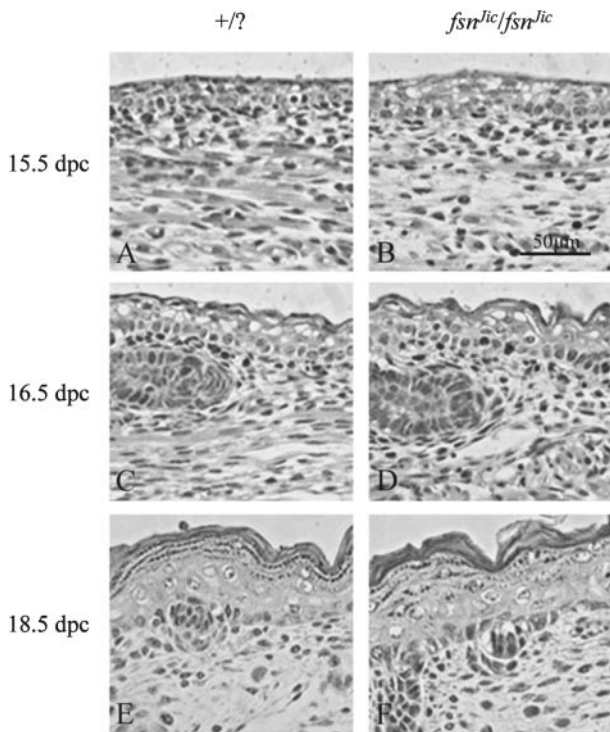


Fig. 5. Skin of *fsn^{Jic}* homozygous embryos at 15.5, 16.5 and 18.5 dpc.

fsn^{Jic} homozygotes indicates an increase in the number of erythroblasts. The cause of the enlarged hearts in *fsn^{Jic}* homozygotes is unknown. As shown in Table 2, peripheral blood collected from *fsn^{Jic}* homozygotes showed increases of nucleated cells (including erythroblasts and WBC) and PLT and reductions in Hct and RBC. It has been reported that *fsn* homozygotes show increases of B cells, macrophages, mast cells, eosinophils and immature erythroid cells (erythroblasts and reticulocytes) and decreases of T cells, lymphocytes, monocytes, neutrophils and mature RBC [2, 12]. These results suggest that *fsn* homozygotes have abnormal differentiation of hematopoietic stem cells.

In order to study hemopoiesis of *fsn^{Jic}* homozygotes, we focused on the phenotypes of B6.INT-*fsn^{Jic}* mice at various embryonic stages. As shown in Fig. 5, skin of *fsn^{Jic}* homozygotes stained with HE did not show any disorders at any embryonic stage. Normal distribution of cytokeratins, epithelial cell markers in the skin of *fsn^{Jic}* homozygous embryos, was also observed (Fig. 6). In contrast, peripheral blood of *fsn^{Jic}* homozygotes in the early embryonic stages already showed abnormali-

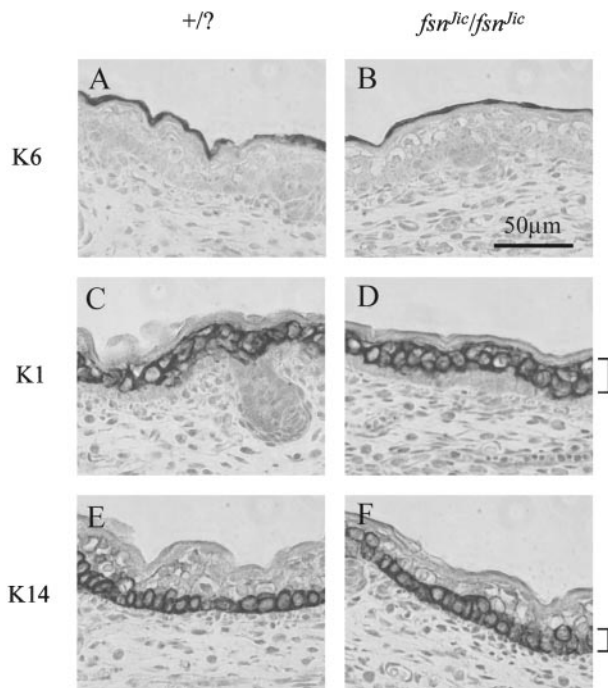


Fig. 6. Immunohistochemical detection of keratinocyte markers on skin of 18.5 dpc embryos. (A) Periderm of normal embryos stained for K6. (B) Periderm of *fsn^{Jic}* homozygous embryos stained for K6. (C) Non-cornified epidermis and stratum spinosum of normal embryos stained for K1. (D) Non-cornified epidermis and stratum spinosum of *fsn^{Jic}* homozygous embryos stained for K1. (E) Epidermis and stratum basale of normal embryo stained for K14. (F) Epidermis and stratum basale of *fsn^{Jic}* homozygous embryo stained for K14.

ties as seen in Fig. 4.

Expressions of *Hbb-bhl* (hemoglobin Z, beta-like embryonic chain) and *Hbb-bl* (hemoglobin, beta adult major chain) genes were studied using RNA extracted from livers of 14.5 dpc embryos in order to observe maturity of erythrocytes [8] in *fsn^{Jic}* homozygous embryos. Both genes were expressed in livers of normal and *fsn^{Jic}* homozygous embryos (data not shown). It was demonstrated in this study that erythrocytes of *fsn^{Jic}* homozygous embryos matured with incomplete enucleation. It is evident that RBC of *fsn^{Jic}* homozygotes may fail to enucleate after switching from primitive hematopoiesis to definitive hematopoiesis, but the mechanisms of enucleation are still not well understood. Kawane *et al.* [7] reported that definitive erythropoiesis requires DNase II secreted from macrophages at the site of definitive erythropoiesis in the mouse fetal liver.

Although the relation between DNase II and *fsn* genes is not known, the *fsn* mutation may be useful in studies of the mechanism of enucleation in RBC.

Transplantation of bone marrow cells obtained from adult *fsn* homozygotes to normal recipient mice resulted in skin lesions and abnormal blood cells. Abnormal phenotypes in skin of *fsn* homozygotes at the postnatal stage have been explained by immunological defects [12, 18]. These results suggest that pleiotropisms observed in *fsn* homozygotes are caused by functional defects of hematopoietic progenitor cells [14, 17]. However, in this study we observed time differences in the appearance of abnormal phenotypes of blood and skin of *fsn^{Jic}* homozygous embryos, therefore, it is possible that abnormal phenotypes observed in various tissues and organs of *fsn* homozygotes are caused by *fsn* gene dysfunction occurring not only in hematopoietic progenitor cells but also in various tissues and organs at different developmental stages.

White *et al.* [17] reported that the hereditary erythroblastic anemia (*hea*) mutation is an allele of the *fsn* locus. The *hea* mutation arose spontaneously in the CFO strain at the Central Institute for Experimental Animals (Kawasaki, Japan) [13]. Three *fsn* mutations, *fsn*, *fsn^{Jic}* and *hea*, which were independently discovered, should be useful for etiological studies of anemia and skin disorders.

Acknowledgments

The authors wish to thank Drs. Satoshi Baba and Yasuhisa Naito (Hamamatsu University School of Medicine) for helpful discussions during the course of this work.

References

1. Beamer, W.G., Maltais, L., and Bernestein, S. 1986. Disturbed iron metabolism in flaky skin (*fsn*) mutant mice. *The Jackson Lab. Ann. Report* 1986; 92.
2. Beamer, W.G., Pelsue, S.C., Shultz, L.D., Sundberg, J.P., and Barker, J.E. 1995. The flaky skin (*fsn*) mutation in mice: map location and description of the anemia. *Blood* 86: 3220–3226.
3. Endo, F., Katoh, H., Yamamoto, S., and Matsuda, I. 1991. A murine model for type III tyrosinemia: lack of immunologically detectable 4-hydroxyphenylpyruvic acid dioxygenase enzyme protein in a novel mouse strain with hypertyrosinemia. *Am. J. Hum. Genet.* 48: 704–709.

4. Endo, F., Awata, H., Katoh, H., and Matsuda, I. 1995. A nonsense mutation in the 4-hydroxyphenylpyruvic acid dioxygenase gene (*Hpd*) causes skipping of the constitutive exon and hypertyrosinemia in mouse strain III. *Genomics* 25: 164–169.
5. Katoh, H. 1989. Animal models derived from the ICR for human disease (in Japanese). *Medical Immunology* 17: 353–361.
6. Katoh, H., Endo, F., Suzuki, K., and Matsuda, I. 1991. Hereditary hypertyrosinemia mouse. *Mouse Genome* 89: 572.
7. Kawane, K., Fukuyama, H., Kondoh, G., Takeda, J., Ohsawa, Y., Uchiyama, Y., and Nagata, S. 2001. Requirement of DNase II for definitive erythropoiesis in the mouse fetal liver. *Science* 292: 1546–1549.
8. Keller, G., Kennedy, M., Papayannopoulou, T., and Wiles, M.V. 1993. Hematopoietic commitment during embryonic stem cell differentiation in culture. *Mol. Cell Biol.* 13: 473–486.
9. Makino, S., Kunimoto, K., Muraoka, Y., Mizushima, Y., Katagiri, K., and Tochino, Y. 1980. Breeding of a non-obese, diabetic strain of mice. *Jikken Dobutsu*. 29: 1–13.
10. Mazzalupo, S. and Coulombe, P.A. 2001. A reporter transgene based on a human keratin 6 gene promoter is specifically expressed in the periderm of mouse embryos. *Mech. Dev.* 100: 65–69.
11. Pelsue, S.C., Schweitzer, P.A., Beamer, W.G., and Shultz, L.D. 1995. Mapping of the flaky skin (*fsn*) mutation on distal mouse chromosome 17. *Mamm. Genome* 6: 758.
12. Pelsue, S.C., Schweitzer, P.A., Schweitzer, I.B., Christianson, S.W., Gott, B., Sundberg, J.P., Beamer, W.G., and Shultz, L.D. 1998. Lymphadenopathy, elevated serum IgE levels, autoimmunity, and mast cell accumulation in flaky skin mutant mice. *Eur. J. Immunol.* 28: 1379–1388.
13. Shimizu, K., Keino, H., Ogasawara, N., and Esaki, K. 1983. Hereditary erythroblastic anaemia in the laboratory mouse. *Lab. Anim.* 17: 198–202.
14. Sundberg, J.P., Boggess, D., Sundberg, B.A., Beamer, W.G., and Shultz, L.D. 1993. Epidermal dendritic cell populations in the flaky skin mutant mouse. *Immunol. Invest.* 22: 389–401.
15. Sundberg, J.P., Boggess, D., Shultz, L., and Beamer, W.G. 1994. The flaky skin (*fsn*) mutation. pp. 253–268. In: (Sundberg J eds) *Handbook of Mouse Mutations with Skin and Hair Abnormalities*. Ann Arbor, MI, CRC Press,
16. Takabayashi, S., Sasaoka, Y., Yamashita, M., Tokumoto, T., Ishikawa, K., and Noguchi, M. 2001. Novel growth factor supporting survival of murine primordial germ cells: evidence from conditioned medium of *ter* fetal gonadal somatic cells. *Mol. Reprod. Dev.* 60: 384–396.
17. White, R.A., McNulty, S.G., Roman, S., Garg, U., Wirtz, E., Kohlbrecher, D., Nsumu, N.N., Pinson, D., Gaedigk, R., Blackmore, K., Copple, A., Rasul, S., Watanabe, M., and Shimizu, K. 2004. Chromosomal localization, hematological characterization, and iron metabolism of the hereditary erythroblastic anemia (*hea*) mutant mouse. *Blood* 104: 1511–1518.
18. Withington, S., Maltby-Askari, E., Welner, R., Parker, R., and Pelsue, S.C. 2002. Antinuclear autoantibodies in flaky skin (*fsn*) mutant mice. *Autoimmunity* 35: 175–181.